AWARD NUMBER: W81XWH-16-1-0428

TITLE: Biochemical Consequences of Cdkal1 Mutations That Result in Unprocesse

PRINCIPAL INVESTIGATOR: Paul F. Agris

CONTRACTING ORGANIZATION: Duke University School of Medicine

REPORT DATE: JUNE 2021

TYPE OF REPORT: Final

PREPARED FOR: U.S. Army Medical Research and Development Command
Fort Detrick, Maryland 21702-5012

DISTRIBUTION STATEMENT: Approved for Public Release;
Distribution Unlimited

REPORT DOCUMENTATION PAGE

Form Approved
OMB No. 0704-0188

1. REPORT DATE	2. REPORT TYPE	3. DATES COVERED
JUNE 2021	Final	08-01-2016 to 02-28-2021

4. TITLE AND SUBTITLE

Biochemical Consequences of Cdkal1 Mutations That Result in Unprocessed, Nonfunctional Insulin and Type 2 Diabetes

5a. CONTRACT NUMBER
W81XWH-16-1-0428

5b. GRANT NUMBER
W81XWH-16-1-0428

5c. PROGRAM ELEMENT NUMBER

6. AUTHOR(S)

Paul F. Agris

E-Mail:

5d. PROJECT NUMBER

5e. TASK NUMBER

5f. WORK UNIT NUMBER

7. PERFORMING ORGANIZATION NAME(S) AND ADDRESS(ES)

Duke University School of Medicine
2200 W MAIN ST STE 710
DURHAM NC 27708-4677FACILITY

8. PERFORMING ORGANIZATION REPORT NUMBER

9. SPONSORING / MONITORING AGENCY NAME(S) AND ADDRESS(ES)

U.S. Army Medical Research and Development Command
Fort Detrick, Maryland 21702-5012

10. SPONSOR/MONITOR'S ACRONYM(S)

11. SPONSOR/MONITOR'S REPORT NUMBER(S)

12. DISTRIBUTION / AVAILABILITY STATEMENT

Approved for Public Release; Distribution Unlimited

13. SUPPLEMENTARY NOTES

14. ABSTRACT

Human Genome Wide Association Studies found a significant risk of Type 2 Diabetes Mellitus (T2DM) in single nucleotide polymorphisms in the cdkal1 gene. The cdkal1 gene is remote from the insulin gene and with the surprising function of a specific tRNA modification. Population studies and case control studies acquired evidence of the connection between Cdkal1 protein and insulin production over the years. To obtain biochemical proofs directly linking potential SNPs to their roles in insulin production and availability is challenging, but the development of Cdkal1 knock out mice and knock out cell lines made it possible to extend our knowledge towards therapeutic field of diabetic research. We produced and characterized a knock down of the cdkal1 gene using small interfering and short hairpin RNA in the NIT-1 cell line, a β-cell line inducible for insulin. The knock down resulted in reduced levels of cdkal1 and mature insulin mRNAs, increased the level of precursor insulin mRNA, decreased Cdkal1 and insulin proteins, and diminished modification of tRNALys3 from t6A37 to ms2t6A37, the specified function of Cdkal1. We further determined that tRNALys3 lacking ms2- is incapable of establishing hydrophobic stabilization to decode the wobble codon AAG.

15. SUBJECT TERMS

Type 2 Diabetes Mellitus

16. SECURITY CLASSIFICATION OF:			17. LIMITATION OF ABSTRACT	18. NUMBER OF PAGES	19a. NAME OF RESPONSIBLE PERSON
a. REPORT	b. ABSTRACT	c. THIS PAGE			USAMRDC
Unclassified	Unclassified	Unclassified	Unclassified	11	19b. TELEPHONE NUMBER *(include area code)*

TABLE OF CONTENTS

1. INTRODUCTION: Human Genome Wide Association Studies found a significant risk of Type 2 Diabetes Mellitus (T2DM) in single nucleotide polymorphisms in the *cdkal1* gene. The *cdkal1* gene is remote from the insulin gene and with the surprising function of a specific tRNA modification. Population studies and case control studies acquired evidence of the connection between Cdkal1 protein and insulin production over the years (Figure 1). To obtain biochemical proofs directly linking potential SNPs to their roles in insulin production and availability is challenging, but the development of Cdkal1 knock out mice and knock out cell lines made it possible to extend our knowledge towards therapeutic field of diabetic research. We produced and characterized a knock down of the *cdkal1* gene using small interfering and short hairpin RNA in the NIT-1 cell line, a β-cell line inducible for insulin (**Major Task 1**). The knock down resulted in reduced levels of *cdkal1* and mature insulin mRNAs, increased the level of precursor insulin mRNA, decreased Cdkal1 and insulin proteins, and diminished modification of $tRNA^{Lys3}$ from t^6A_{37} to $ms^2t^6A_{37}$ (**Major Task 2**), the specified function of Cdkal1 (**Major Task 3**, manuscript publication). We further determined that $tRNA^{Lys3}$ lacking ms^2- is incapable of establishing hydrophobic stabilization to decode the wobble codon AAG.

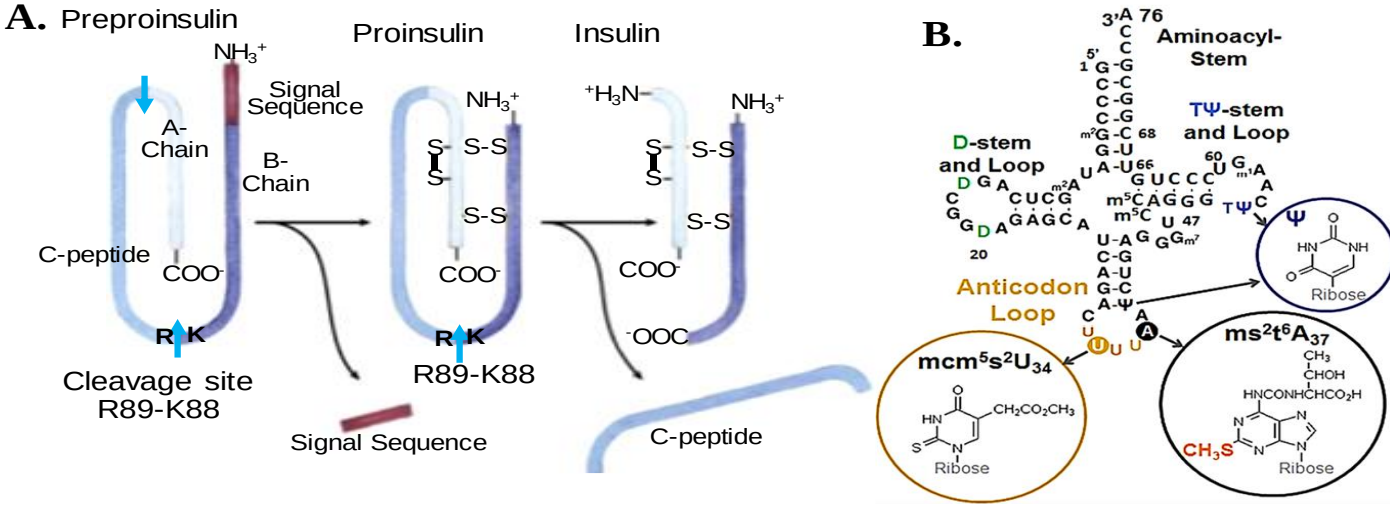

Figure 1. A. Human Insulin Processing. Insulin mRNA is translated into one peptide that will undergo cleavage and linkages via disulfide bridges. One of two important cleavage sites is K88-R89. A preproinsulin mRNA necessitates $tRNA^{Lys3}$ (B.) with its fully modified anticodon loop nucleosides to accurately read the Lys AAG codon. The resulting peptide is composed of a signal sequence, A-chain, B-chain and C-peptide, the A- and B-chain associate into mature insulin. **B. Human $tRNA^{Lys3}$.** $tRNA^{Lys3}$ decodes AAA and AAG in mRNA on the ribosome. The **ms^2-** modification of t^6A_{37} results in $ms^2t^6A_{37}$ and is the product of Cdkal1 enzymatic activity. The modification $ms^2t^6A_{37}$ facilitates accurate and efficient decoding of the lysine codons. Domains are labeled. Anticodon loop modified nucleosides positions and structures are circled. The **ms^2-** modification made by Cdkal1 is found with $ms^2t^6A_{37}$. The anticodon 5'-adjacent invariant U and 3'-modified adenosine are noted.

2. KEYWORDS: Type 2 Diabetes; Cdkal1; tRNA modification; Decoding on the ribosome; Cdkal1 protein; insulin

3. ACCOMPLISHMENTS:

What were the major goals of the project?

Aim 1: Conclude experiments for revision of manuscript

Major Task 1: Characterize new murine knockout of *cdkal1* in a murine β-cell line.

Major Task 2: Isolate and characterize modifications of $tRNA^{Lys3}$

Major Task 3: Submit manuscript revision

<u>Aim 2:</u> Edit galley Proofs and resubmit

What was accomplished under these goals?

1) Major activities:

a. We characterized NIT-1 *cdkal1* knock down β-cells in culture as to their production of Cdkal and insulin. Characterization of a new murine knock**out** of *cdkal1* in a murine β-cell line was begun.

b. tRNA was isolated and characterized for modifications of $tRNA^{Lys3}$ particularly t^6A and ms^2t^6A.

c. A manuscript was revised re-submitted, accepted, galley proofs corrected and published.

2) Specific objectives:
Cdkal1 knockout cell line validation with assessing *cdkal1* mRNA and Cdkal1 protein production.
Assessment of insulin mRNA and protein populations
Rescue *cdkal1*-deficient cells with transfection of human cDNA *cdkal1*.
MS analysis of insulin from Cdkal1 deficient and rescued cells
Design and purchase oligo probes to isolate $tRNA^{Lys3}$
Isolate $tRNA^{Lys3}$ from *cdkal1*-deficient and *cdkal1* rescued cells and have modified nucleosides identified with HPLC/MS

Revise manuscript as suggested by reviewers
Submit revised manuscript
Have all 11 authors contribute editing
Compile edits and apply
Submit edited galleys

3) **Significant results or key outcomes, including major findings, developments, or conclusions (both positive and negative):** The NIT-1 cell line (ATCC® CRL-2055™) is inducible for insulin production with high glucose concentrations, theophylline and KCl (Figure 2A). The cells were stimulated to produce insulin with Theophylline (10 mM with 5.5 mM glucose) or KCl (40 mM) in SF media (Figure 2A). In order to determine the effect of a reduced Cdkal1 protein production, we knocked down *cdkal1* gene expression with two distinct methods. The *cdkal1* gene was knocked down by transfection of an esiRNA (endonuclease-prepared siRNA, 30, 50 or 70 nM using Lipofectamine, LF*;* Sigma) and by a Lentiviral shRNA (Sigma). Cells were also transfected with a control GFP esiRNA in antibiotic-free medium (6 h). Cells were glucose starved overnight in SF-DMEM, and induced for insulin (90 min) or left unstimulated (SF-DMEM with 600 KIU/mL aprotinin). Cells transfected with a control GFP esiRNA or Lipofectamine (LF RNAiMax reagent) alone responded to stimulation similar to cells that had not been transfected. Supernatants of *cdkal1* esiRNA (50 nM) knockdown cells assayed for insulin by ELISA had as low as 20% of the mature insulin production compared to a control esiRNA and LF-transfected cultures (Figure 2B). The cells were lysed in RIPA buffer with protease inhibitors and the lysates were processed for Western blots that showed decreased Cdkal1 protein as well as decreased insulin production (Supplemental Figure 1).

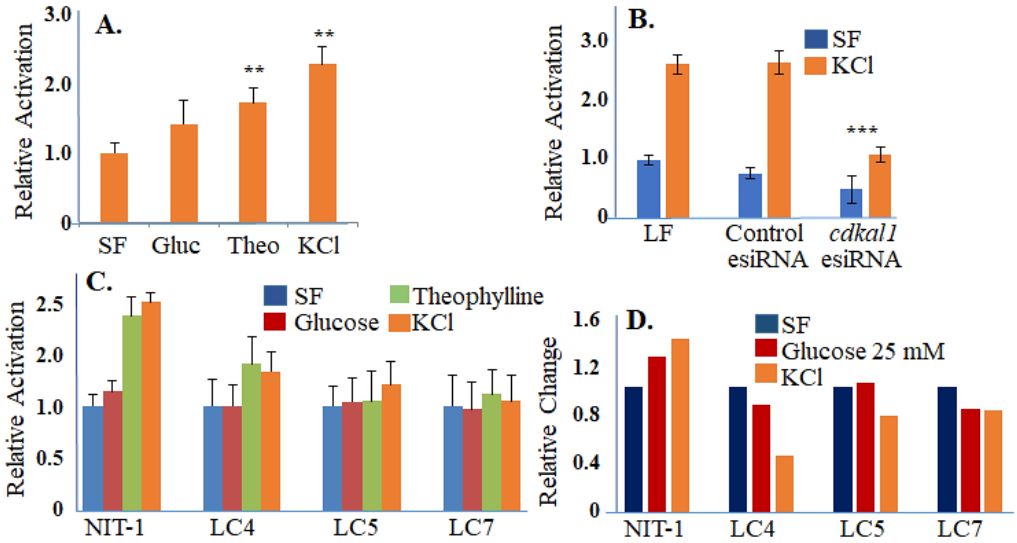

Figure 2. A. Relative activation of insulin produced in stimulated NIT-1 cells. NIT-1 cells plated in 24 wells for 48 h were serum starved overnight and stimulated for 90 mins with control (SF), Glucose (25 mM), Theophylline (10 mM in Glu 5.5), and KCl (40 mM) in SF medium with Aprotinin. **A. Insulin secretion in cell supernatants** was measured by ELISA using a mouse proinsulin and insulin antibody and concentration calculated using a human insulin protein standard curve. Insulin levels were normalized to control cells and expressed as fold-change over control (Relative Activation). Results are an average three biological experiments. **- indicates p value <0.01 using a Students t-test. **B. Insulin levels in supernatants from NIT-1 knockdown cells.** Secreted insulin levels from esiRNA-transfected (50 nM with LF 1 µl) NIT-1 cells were measured by ELISA following stimulation with KCl or Serum-free medium. Data is expressed as Relative Activation compared to unstimulated (SF) Lipofectamine RNAiMAx (LF) - only transfected control cells. ***- indicates p value <0.001 using a Students t-test. **C. Secreted insulin levels** from Lentiviral shRNA knockdown clones of NIT-1 cells (LC4, LC5 and LC7) were measured by ELISA following stimulation. Data is expressed as Relative Activation compared to non-stimulated control cells of each cell type. Experiments were controlled for the amounts of protein. **D. Insulin protein levels in esiRNA knockdown cell lysates**. Protein levels were normalized to GAPDH and expressed as Relative Densitometric Units (RDU).

Cells were also infected with four different Lentiviral shRNA constructs against the *cdkal1* gene in antibiotic-free medium and selected with puromycin (3.5 µg). Clones, LC4, LC5, and LC7 that survived puromycin selection were

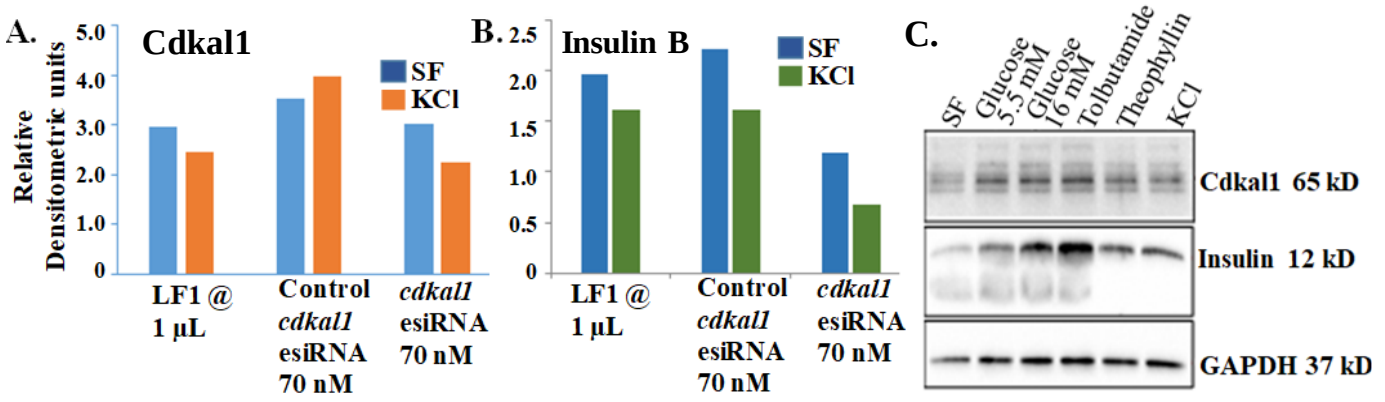

Figure 3. Insulin B protein and Cdkal1 protein in NIT-1 knockdown cell lysates. Western blots were employed to identify levels of insulin, Cdkal1 and control GAPDH proteins in Control esiRNA (70 nM) and *cdkal1* esiRNA knockdown cells unstimulated (Serum Free, SF) and stimulated (KCl) to produce insulin. **A.** Cdkal1 levels in control LF and GFP esiRNA cells stimulated and not stimulated to produce insulin and in *cdkal1* esiRNA (70 nM) knockdown cells. **B.** Insulin B protein levels in control LF and GFP esiRNA-treated cells stimulated and not stimulated to produce insulin and in *cdkal1* esiRNA (70 nM) knockdown cells. **C.** Mouse antibodies were used in Western blots against Insulin B and Cdkal1 or GAPDH. Insulin production was induced by low and high glucose, Tolbutamide, Theophyllin and KCl. Protein levels in cell lysates in Western blots were quantitated with Image J software and normalized to GAPDH levels and expressed as fold-change from control unstimulated (SF) cell lysates. LF – Lipofectamine (1ul); Control *GFP*-esiRNA 70 nM; *cdkal1*-esiRNA 70 nM. Protein (250 µg) was loaded on SDS-PAGE gels and immune blotted using mouse antibodies against Insulin B (Clone C-12, Santa Cruz), Cdkal1 (clone E9, Santa Cruz), or GAPDH (Clone MA5-GA1R, Thermo Fisher). GAPDH was used as a loading control.

expanded and DNA isolated and sequenced. Insulin induced cells were analyzed with the GSIR assay, ELISA and Western blot. Compared to normal NIT-1 cells, the secreted insulin levels were 50% or lower with stimulation by Theophylline and KCl (Figure 2C). When cell lysates were assayed for insulin, LC4 stimulated by KCl showed that the knockdown of *cdkal1* by the shRNA construct inhibited insulin production by >60% (Figure 2D). Analysis of stimulated NIT-1 cell lysates by Western blotting showed no significant changes in the levels of Cdkal1 protein in normal NIT-1 cells although knockdown cells had lower Cdkal1 protein levels (Figure 3). The amount of GAPDH control protein was not affected in the Cdkal1 deficient cells.

The function of Cdkal1 protein's modification of tRNA is accurate and efficient translation of AAG/AAA codons. Insulin mRNA requires the Cdkal1 modification of $tRNA^{Lys3}$ from t^6A_{37} to $ms^2t^6A_{37}$ for insertion of lysine at position 88. A significant decrease was observed in ms^2t^6A relative to t^6A in RNA (<200 nts) isolated from cells that had been knocked down (Figure 4). We isolated RNA from esiRNA knockdown cells, stimulated and unstimulated for insulin production and control Lipofectamine only (LF) cells. The RNA was fractionated so that we could analyze small RNAs less than 200 nucleotides such as tRNAs without rRNA present (Ambion *mir*Vana miRNA Isolation Kit). The RNA was hydrolyzed to nucleosides and the modified nucleoside analysis conducted by UHPLC-MS/MS (triple quadrupole MS (Waters MS).[16] The ms^2t^6A modification decreased in tRNAs from esiRNA30 and esiRNA50 knockdown cells. As expected, the decrease was most dramatic in tRNA from esiRNA50 cells grown in SF medium, and less so when the cells were stimulated by KCl. The decrease of ms^2t^6A in tRNA is consistent with and probably the cause of a decrease in secreted insulin and increase in precursor insulin mRNA.

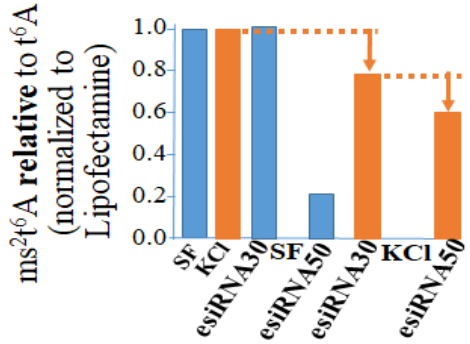

Figure 4. The ms^2t^6A modification is diminished in tRNA from *cdkal1* esiRNA knockdown cells. The modified nucleosides in small RNA purified from esiRNA30 and esiRNA50 knockdown cells and control LF cells were hydrolyzed to nucleosides and analyzed by UHPLC-MS/MS. The results are presented as the amount of ms^2t^6A relative to ms^2t^6A plus t^6A ($ms^2t^6A/ms^2t^6A + t^6A$) normalized to LF controls. Initially the concentrations of ms^2t^6A and t^6A were determined relative to the major nucleoside A. The results are the average of three biological assays conducted by two different institutions. **LF** - control cells transfected with Lipofectamine only; **esiRNA30** and **50** - Cdkal1 knockdown cells transfected with 30 and 50 nM esiRNA. **SF** – control cells serum-free; **KCl** – 4 mM KCl

Large sequence RNA was isolated from normal and transfected knockdown NIT-1 cells (Qiagen RNEasy Plus kit) and rRNA was removed (Qiagen RNEasy MinElute Kit). Quantitative real-time PCR was conducted to determine the presence of *cdkal1*, precursor insulin, and mature insulin mRNAs.[17] Threshold Cq values were normalized to actin levels. Relative expression was calculated using the $2^{\Delta\Delta Cq}$ method.[18] The expression of *cdkal1* mRNA levels

increased by ~60% in normal NIT-1 cells following stimulation with KCl (Figure 5A). However, in stimulated *cdkal1*-esiRNA treated knockdown cells, the mRNA levels were decreased by ~30% (Figure 5B). To determine the regulation of insulin transcription, we applied a unique strategy using two sets of primers that amplified total mouse insulin I and II mRNA (fully processed mature insulin mRNA) and a precursor mRNA species containing intron 2 (Figure 5C).[17] The levels of mature mRNA and precursor mRNA insulin levels were quantitated and expressed as the real time threshold cycle (C_T) values, in untreated (SF) and KCl stimulated NIT-1 normal or knockdown cells. Although no differences were seen in mature insulin mRNA levels, significant changes in precursor insulin mRNA levels were detected with stimulation to produce insulin (Figure 5D). When the abundance of precursor insulin mRNA relative to mature insulin mRNA in control cells is normalized to 1.00, in stimulated *cdkal1* knockdown cells the ratio is 1.95 relative to mature insulin mRNA. In β-cells when the *cdkal1* gene is non-functional or missing and the $tRNA^{Lys3}$ modification ms^2t^6A has decreased, *cdkal1* mRNA has decreased 30% also. However, the insulin precursor mRNA is significantly increased. Thus, *cdkal1* knockdown cells stimulated to produce insulin are yet secreting less mature insulin. Lysates from these cells exhibited significantly decreased insulin and proinsulin.

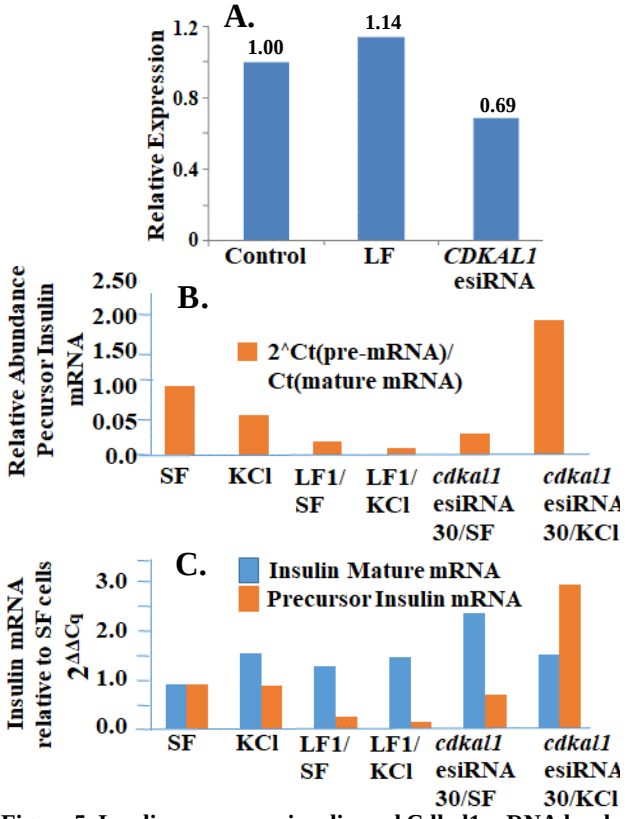

Figure 5. Insulin, precursor insulin and Cdkal1 mRNA levels in *cdkal1* esiRNA knockdown cells. A. Insulin mRNA is increased with stimulation in normal NIT-1 cells. **B.** Mature insulin mRNA is significantly reduced in KCl stimulated knockdown cells. mRNA levels were normalized to actin mRNA and expressed as fold-change to Control normal NIT-1 cells. LF cells - transfected with Lipofectamine only, esiRNA30 - transfected with esiRNA 30 nM. In *cdkal1*-esiRNA treated knockdown cells, the mRNA levels were reduced by ~30%. Threshold Cq values were normalized to actin levels. Relative expression was calculated using the $2^{\Delta\Delta Cq}$ method. **C.** The insulin mature (blue) and precursor (orange) mRNA levels were assessed with RT-qPCR. RNA isolated from normal or knockdown NIT-1 cells following stimulation for insulin production. The 2-step RT-qPCR method was used to determine the expression levels of insulin mRNA. Threshold Cq values were normalized to actin levels. Expression relative to SF mRNA levels was calculated using the $2^{\Delta\Delta Cq}$ method.

We asked why should the modification ms^2- play such an important role in $tRNA^{Lys3}$ in translating the lysine wobble codon AAG in insulin mRNA? When the anticodon $U_{34}U_{35}U_{36}$ with the adjacent $ms^2t^6A_{37}$ binds the wobble codon G3A2A1, the $ms^2t^6A_{37}$ is three nucleosides distant from the U_{34}:G3 pair. There are three posttranscriptional modifications in the anticodon stem and loop (ASL) of $tRNA^{Lys3}$, 5-methoxycarbonylmethyl-2-thiouridine at wobble position 34 ($mcm^5s^2U_{34}$), 2-methylthio-*N*^{6}-threonylcarbamoyladenosine at position 37 ($ms^2t^6A_{37}$) adjacent to the anticodon and pseudouridine (Ψ_{39}) at position 39 in the stem. The fully modified $ms^2t^6A_{37}$ and $mcm^5s^2U_{34}$ are required to achieve wild-type binding activity of human $tRNA^{Lys3}$ to AAA and the wobble codon AAG. NMR structure determination and molecular dynamics simulations (MDS) of the ASL demonstrated that the ms^2t^6- modification of A_{37} supports the anticodon nucleoside stack 5' to 3' and reduces solvent accessibility of U_{36}.

To explore the role of the $tRNA^{Lys3}$ modifications at A_{37} for recognition and decoding, we performed molecular simulations of the anticodon stem-loop of the tRNA (ASL) bound to the mRNA AAG at the A site of the eukaryotic ribosome. We compared three simulations with the ASL-$mcm^5s^2U_{34}$ with A_{37}, t^6A_{37}, and $ms^2t^6A_{37}$ each bound to the wobble codon AAG on the ribosome. First, we considered the effect of the modifications on the codon-anticodon interaction. We compared the hydrogen bonding between the codon and anticodon nucleosides (A1:U_{36}, A2:U_{35} and G3:$mcm^5s^2U_{34}$), in the three systems (Figure 6). Interestingly, we observe that the hydrogen bonding is stronger for all three positions of the codon-anticodon base pairs by the addition of the t^6-modification to A_{37} and is further enhanced by the addition of the ms^2- to t^6A_{37}. Remarkably, we find that this enhancement is most pronounced when the $mcm^5s^2U_{34}$:G_3 base-pair is considered, which is the farthest from the A_{37}.

Next, we asked how does the modification at A_{37} lead to significant strengthening of codon anticodon base-pairing? The dominant locations of the threonylcarbamol-group in both t^6A_{37} & $ms^2t^6A_{37}$ systems has the hydrophilic moieties of the modification (carboxyl and hydroxyl groups) either pointing away from the ASL cavity and remaining well hydrated or are involved in a cross-loop interaction with the backbone (2' hydroxyl group) of C_{32} (Figure 7A). The rest of the modification fits inside the ASL cavity through hydrophobic and hydrogen bonding interactions, thereby offering stability to the neighboring codon-anticodon base-pairs. Furthermore, we observed transient interaction between the terminal methyl groups of $ms^2t^6A_{37}$ and $mcm^5s^2U_{34}$ (Figure 7B), suggesting that the enhancement in stability due to the modification at A_{37} extends to the codon-anticodon base pair farthest from A_{37}. Most interestingly, we also found that the t^6- group interaction with the ASL cavity is more stable with the addition of the ms^2- group. The ms^2-group boosts the stacking interaction between A_{37} and the A1 codon of which the threonylcarbamoyl-group is held steady in the ASL cavity. Overall, our molecular simulations reveal a cascading mechanism for $ms^2t^6A_{37}$, in which hydrogen bonding energy and the hydrophobic interactions of base-stacking by the methylthio-group stabilizes the threonylcarbamoyl-group in the ASL cavity. This in turn facilitates the hydrophobic interaction of the threonyl-carbamoyl-group with the methyl-carboxymethyl- (mcm^5-) group on U_{34} three nucleosides away, stabilizing the codon-anticodon base-pairing at the wobble position for wobble codon AAG recognition.

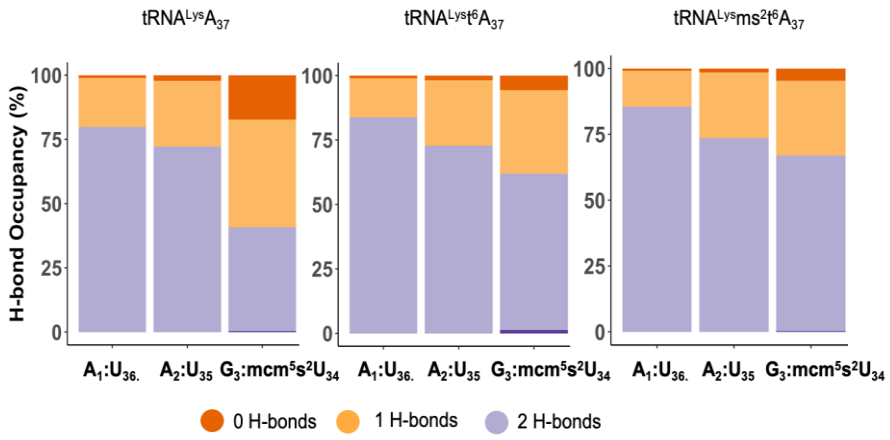

Figure 5. The hydrogen bond occupancy for the $tRNA^{Lys3}$ anticodon-codon base pairs. The hydrogen bond (H-bond) occupancy for the $tRNA^{Lys3}$ anticodon-codon base pairs for the $mcm^5U_{34}U_{35}U_{36}$ anticodon interacting with the $A_1A_2G_3$ wobble codon for the three cases of $tRNA^{Lys3}$-A_{37}, $tRNA^{Lys3}$-t^6A_{37} and $tRNA^{Lys3}$-$ms^2t^6A_{37}$. The chart presents the H-bond occupancy for the percentage of the simulation time the base-pairs, A1:U_{36}, A2:U_{35}, G3:$mcm^5s^2U_{34}$ interact and establish 0, 1, or 2 H-bonds.

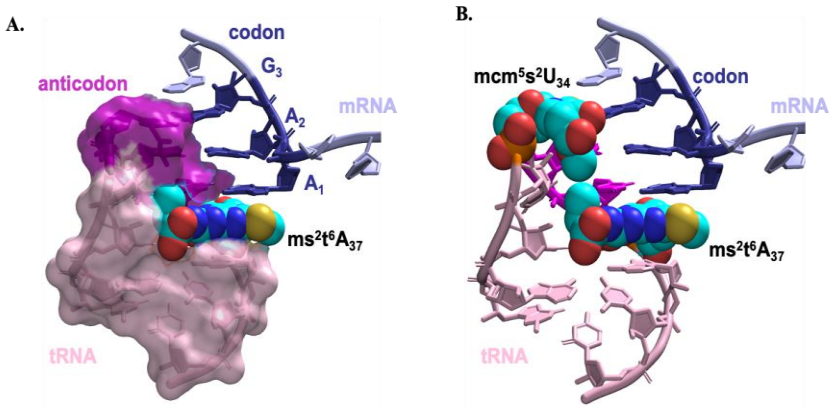

Figure 7. The dominant orientation of the hypermodified $ms^2t^6A_{37}$ shown in space filling model interacting with the anticodon stem loop cavity. **A**. The terminal carboxyl group of the threonylcarbamoyl-group faces away from the ASL cavity, while the aliphatic carbons and the terminal methyl group fill up the cavity. Stacking between A1, A_{37} and A_{38} is enhanced by the addition of the thiomethyl-group to t^6A_{37}, $ms^2t^6A_{37}$. **B.** The interaction between hypermodified $ms^2t^6A_{37}$ and $mcm^5s^2U_{34}$ shown in space filling model. Hydrophobic contacts between the two modified nucleotides assists $mcm^5s^2U_{34}$ in maintaining the anticodon:codon interaction at the wobble position.

Other achievements: Why does $tRNA^{Lys3}$ with the fully modified $ms^2t^6A_{37}$ decode the lysine wobble codon AAG-88 in β-cells, whereas $tRNA^{Lys3}$ lacking the fully modified $ms^2t^6A_{37}$ in cells deficient of Cdkal1 protein does not decode AAG? In humans, there are three lysine isoaccepting tRNAs that decode the lysine codons AAG and AAA. However, only $tRNA^{Lys3}$ with the anticodon composed of an extensively modified 5-methoxycarbonyl-2-thio-U_{34}-UU_{36} is able to decode AAA and also decode its wobble codon AAG. The other two lysine isoaccepting tRNAs have anticodons that are unmodified, C_{34}-UU. The relative amounts of the three tRNA species in β-cells are unknown. Codon binding analyses have shown that the 5-methoxycarbonyl-2-thiouridine-34 ($mcm^5s^2U_{34}$) and the $ms^2t^6A_{37}$ are important for decoding AAG. The $ms^2t^6A_{37}$ maintains in the NMR-restrained molecular dynamics derived solution structure, the anticodon in an open loop conformation required for ribosomal binding. With each of the two lysine codons bound into the A site in the 30S ribosomal subunit crystal structures, we observed that the $tRNA^{Lys3}$ modified nucleosides $mcm^5s^2U_{34}$ and $ms^2t^6A_{37}$ participate in the stability of the anticodon/codon

interaction. Without a doubt, the modifications pre-structure the anticodon for effective and accurate recognition of cognate and wobble codons. The ms^2t^6modification of A_{37} is a prerequisite for maintaining this structure and reduces solvent accessibility of U_{36}. Modifications provide functional versatility to the tRNA through changes in chemical and structural environments. However, the way in which the ms^2-modification participates in the AAA and AAG codon recognition is not known, nor is the degree to which the modifications enhance the wobble versus cognate codon binding. We have used molecular dynamic simulations (MDS) to answer these questions, and we have recently found that the binding to the wobble codon AAG is most significantly enhanced by the $ms^2t^6A_{37}$ by hydrophobic interactions and the removal of water molecules between codon and anticodon.

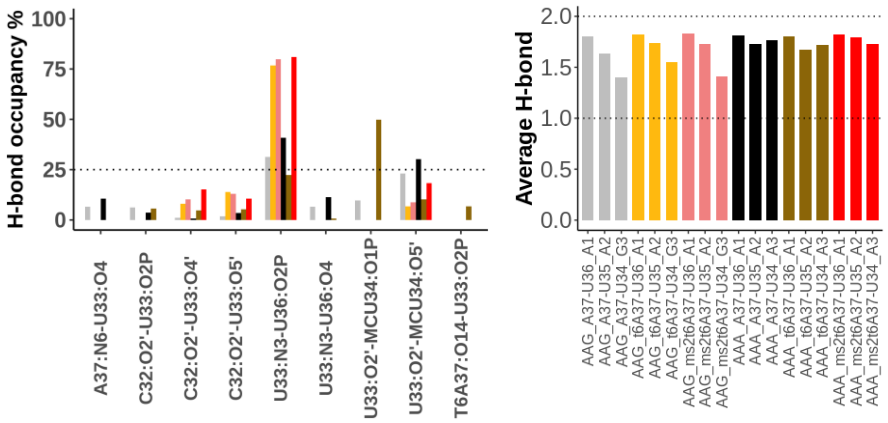

Figure 8. MSD determination of H-bond occupancy for $tRNA^{Lys3}$ with A_{37}, t^6A_{37} or $ms^2t^6A_{37}$ when $tRNA^{Lys3}$ is bound to AAG and AAA. MSD determination of H-bond occupancy was determined for $tRNA^{Lys3}$ bound to AAG or AAA on the eucaryotic ribosome. Left: Percent occupancy (gray is A_{37} with AAG; yellow, AAG with t^6A_{37}; pink, AAG with $ms^2t^6A_{37}$; black, A_{37} with AAA; yellow, AAA with t^6A_{37}; pink, AAA with $ms^2t^6A_{37}$.) Right: Average H-bonding (color code the same.)

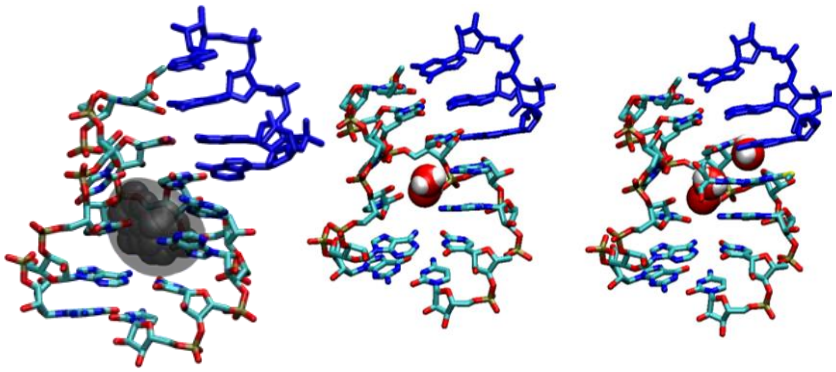

Figure 9. Hydration of $tRNA^{Lys3}$ anticodon bound to codon with t^6A_{37} vs. $ms^2t^6A_{37}$. The anticodon bound to the codon creates a cavity which has a degree of hydration depending on the hydrophobicity of the interaction. MDS show that the $ms^2t^6A_{37}$ is more hydrophobic and repulses water thereby enhancing the modification's ability to cross duplex stack.

Stated goals were not fully met: We did not fully characterize the new murine knockout of *cdkal1* in a murine β-cell line. We wanted to rescue the line with transfection of the **human** *cdkal1*. Description of other pertinent data and graphs: Upon full examination of H-bonds between the codon and anticodon, we found that the average H-bond occupancy was no different for t^6A_{37} and $ms^2t^6A_{37}$ (Figure 8). The modifications t^6A_{37} and $ms^2t^6A_{37}$ provide added H-bond strength but there is no difference between the two. However, the ms^2- group affects the hydration of the ASL:codon helical cavity (Figure 9). Wobble decoding of G_3-U_{34} in the AAG codon by $tRNA^{Lys3}$, benefits from the modifications at both the 34th and the 37th position. The threonyl group of t^6A_{37} stabilizes the conformation of the anticodon stem loop via cross loop interactions with $mcm^5s^2U_{34}$ The methyl-thio group adds additional stability by holding the threonyl group in place, and further dehydrating the ASL.

4) A succinct description of the methodology used: NIT-1 is a β-cell line established from a transgenic mouse with the SV40 large T-antigen. It is grown in Hams F12K medium (F12K with L-Glutamine 90%; heat-inactivated, dialyzed fetal bovine serum 10%, FBS, Sigma; and 1 X penicillin-streptomycin, Invitrogen). Theophylline (10 mM with 5.5 mM glucose), glucose or KCl were used to stimulate insulin production. To knockdown the gene, we transfected an experimental esiRNA (endonuclease-prepared siRNA, Sigma) and a control GFP esiRNA with Lipofectamine 2000 and a Lentiviral shRNA (Sigma).

Stimulation of insulin production. NIT-1 has a glucose stimulated insulin response (GSIR) generated with a high glucose concentration (25 mM) when preceded by overnight incubation in low glucose, serum-free medium (SF-DMEM). Insulin production was assayed by ELISA (mouse proinsulin and insulin antibody, ABClonal)

Transfections. Plated cells were transfected with a control GFP esiRNA or cdkal1 esiRNA (30, 50 or 70 nM using Lipofectamine, LF, RNAiMax reagent, 0.5 or 1 µl, Invitrogen) in antibiotic-free medium (6 h). Cells were then incubated in fresh medium (48 h), serum and glucose starved overnight in SF-DMEM, and induced for insulin (90 min) or left unstimulated (SF-DMEM with 600 KIU/mL aprotinin).

Modified Nucleoside Analysis. Small RNAs (<200 nucleotides) were isolated (Ambion *mir*Vana miRNA Isolation Kit) and the RNA was dialyzed extensively against phosphate buffer (10 mM NaH_2PO_4, pH 6.8) and then against water (18 mΩ). The RNA was hydrolyzed to nucleosides enzymatically rather than chemical digestion. The 2-step process cleaves first the phosphodiester bond with nuclease P1 resulting in nucleoside-5′-monophosphates followed by bacterial alkaline phosphatase (BAP) to cleave the 5′-phosphate from the nucleosides resulting in individual nucleosides and phosphoric acid. The modified nucleoside analysis was conducted by UHPLC-MS/MS (triple quadrupole MS (Waters MS).

RT-qPCR of insulin and *cdkal1* mRNA. We used RT-qPCR to assess the level of expression of mature insulin (mouse insulin I and II) or a pre-insulin or precursor containing intron 2 in normal and in esiRNA transfected NIT-1 cells, induced and not induced for insulin production. Large sequence RNA was isolated from normal and transfected knockdown NIT-1 cells (Qiagen RNEasy Plus kit) and rRNA was removed (Qiagen RNEasy MinElute Kit). A 2-step RT-PCR was conducted to determine the presence of *cdkal1*, precursor insulin, and mature insulin mRNAs (BioRad 2step c-DNA Synthesis kit). The expression and amount of *cdkal1* mRNA was determined by quantitative real-time PCR (RT-qPCR) analysis. Threshold Cq values were normalized to actin levels. Relative expression was calculated using the $2^{\Delta\Delta Cq}$ method.

Molecular Dynamics Simulations. The crystal structure of the mammalian ribosome was obtained from the Protein Data Bank (PDB ID: 5LZS). An intact stable fragment of structure was used for simulations, which included the mRNA, the anticodon stem loop (ASL) of the A-site tRNA, ribosomal RNA and ribosomal proteins within 25 Å of the codon and anticodon minihelix at the A-site. The ASL and the mRNA codon were modified to match the human $tRNA^{Lys3}$ ASL sequence and the lysine codon respectively using MOE. Six different constructs of the ASL:codon pair were modeled with codons AAA and AAG, each paired with the ASL containing the unmodified nucleoside A_{37}, threonylcarbonyladenosine (t^6A_{37}) and hypermodified 2-methylthio N^6-threonylcarbonyl adenosine ($ms^2t^6A_{37}$). In order to simulate the modified tRNA, AMBER type force-field parameters were developed for the atoms of the modified nucleosides – pseudouridineΨ, mcm^5s^2U, t^6A and ms^2t^6A. The geometry of the modified nucleosides was optimized using Hatree-Fock level theory and 6-31G* basis-sets in Webmo. For obtaining the partial charges on the atoms, the online RESP charge-fitting server REDS was used. AMBER-99 force field parameters and AMBER-99 parameters with the Chen-Garcia correction were used for bonded and Lennard-Jones (LJ) interactions, respectively. Molecular dynamics (MD) simulations were performed using Gromacs-2016.4 and Gromacs-2019.6 packages. The MD simulations incorporated a leap-frog algorithm with a 2-fs timestep to integrate the equations of motion. The system was maintained at 300K, using the velocity rescaling thermostat. The pressure was maintained at 1 atm using the Berendsen barostat for equilibration. Long-range electrostatic interactions were calculated using particle mesh Ewald (PME) algorithm with a real space cut-off of 1.0 nm. LJ interactions were truncated at 1.0 nm. The TIP3P model was used to represent the water molecules, and the LINCS algorithm was used to constrain the motion of hydrogen atoms bonded to heavy atoms. The system was subjected to energy minimization to prevent any overlap of atoms, followed by 0.5 ns of equilibration and a 25-ns production run. During simulations, the ribosomal RNA, proteins and the mRNA (except the codon) were held in place using position restraints on the heavy atoms of the RNA and protein backbone with a force constant of 1000 Newton/nm in each spatial dimension for the simulation. Coordinates of the ribosomal fragment (rRNA, tRNA, and mRNA) were stored every 1 ps for further analysis. The simulations were visualized using Visual Molecular Dynamics software and analyzed using tools from Gromacs.

What opportunities for training and professional development has the project provided?

▪ Training activities. The project provided training for postdocs and undergraduate students. They were able to work with Dr. Agris one-on-one to advance skills and experience and assist others in learning.

Postdocs were able to increase knowledge and skill sets, attend conferences, and seminars, and present seminars.

- **How were the results disseminated to communities of interest?**

Results and conclusions were disseminated through the publication and through seminars and poster presentations

- **What do you plan to do during the next reporting period to accomplish the goals?**

Nothing to Report.

IMPACT: *Describe distinctive contributions, major accomplishments, innovations, successes, or any change in practice or behavior that has come about as a result of the project relative to:*

- **What was the impact on the development of the principal discipline(s) of the project?**

Nothing to Report; too early.

- **What was the impact on other disciplines?**

Nothing to Report; too early.

- **What was the impact on technology transfer?**

Nothing to Report; too early.

- **What was the impact on society beyond science and technology?**

Nothing to Report; too early.

CHANGES/PROBLEMS: Changes in approach and reasons for change

Nothing to Report.

Actual or anticipated problems or delays and actions or plans to resolve them

We anticipated that the knockdown would be more effective. We had to move on to a knockout of the endogenous *cdkal1*. The knockouts apparently are almost 100% effective.

Changes that had a significant impact on expenditures

Nothing to Report

Significant changes in use or care of human subjects, vertebrate animals, biohazards, and/or select agents

Nothing to Report

Significant changes in use or care of human subjects. Not applicable

- **Significant changes in use or care of vertebrate animals.** Not applicable
- **Significant changes in use of biohazards and/or select agents.** Not applicable

PRODUCTS: *Cdkal1* knockout cell line.

Publications, conference papers, and presentations

- **Journal publications.**

Narendran Amithi, Vangaveti Sweta, Ranganathan Srivathsan V., Eruysal Emily, Craft Miranda, Alrifai Omar, Chua Fu Yee, Sarachan Kathryn, Litwa Breann, Ramachandran Sheetal, Agris Paul F. Silencing of the tRNA Modification Enzyme Cdkal1 Effects Functional Insulin Synthesis in NIT-1 Cells: tRNALys3 Lacking ms2-(ms2t6A37) is Unable to Establish Sufficient Anticodon:Codon Interactions to Decode the Wobble Codon AAG Frontiers in Molecular Biosciences, 7: 584228. Published online 2021 Feb 9.

Federal support (yes).

Books or other non-periodical, one-time publications. Nothing to Report

Other publications, conference papers, and presentations. Nothing to Report

Website(s) or other Internet site(s) Nothing to Report

Technologies or techniques Nothing to Report

Inventions, patent applications, and/or licenses Nothing to Report

Other Products Nothing to Report**PARTICIPANTS & OTHER COLLABORATING ORGANIZATIONS**

- **What individuals have worked on the project?**

Name:	Amithi Narendran
Project Role:	Lab manager
Researcher Identifier (e.g. ORCID ID):	

Nearest person month worked:	12
Contribution to Project:	Ms. Narendran has performed work in the area of cell culture, knock downs, Wester blots.
Funding Support:	
Name:	Sweta Vangaveti
Project Role:	Senior postdoc
Researcher Identifier (e.g. ORCID ID):	
Nearest person month worked:	9
Contribution to Project:	Dr. Vangaveti conducted MDS and interpretation
Funding Support:	
Name:	Srivathsan V. Ranganathan
Project Role:	Senior postdoc
Researcher Identifier (e.g. ORCID ID):	
Nearest person month worked:	9
Contribution to Project:	Dr. Ranganathan conducted MDS and interpretation
Funding Support:	
Name:	Emily Eruysal, Miranda Craft, Omar Alrifai, Fu Yee Chua, Emily Eruysal, Miranda Craft, Omar Alrifai, Fu Yee Chua,
Project Role:	Undergraduate researchers
Researcher Identifier (e.g. ORCID ID):	
Nearest person month worked:	6
Contribution to Project:	Assay development and application
Funding Support:	

Has there been a change in the active other support of the PD/PI(s) or senior/key personnel since the last reporting period? No

What other organizations were involved as partners?

Nothing to Report.

SPECIAL REPORTING REQUIREMENTS

COLLABORATIVE AWARDS: None.